PROCESSING OF ERS-2 DATA FOR ISTANBUL BY USING NARROW FOCUS AND WIDE FOCUS ALGORITHMS

Cihan Erbaş

e-mail: erbas@ehb.itu.edu.tr
Istanbul Technical University, Faculty of Electrical and Electronics Engineering, Department of Electronics and Communication Engineering, 34469, Maslak, Istanbul, Turkey

Keywords: Synthetic aperture radar,Doppler shift, raw data processing, focusing algorithms

ABSTRACT

In this study synthetic aperture radar (SAR) raw data are processed via various processing algorithms. Characterization of the surface reflectivity pattern is performed. Surface reflectivity pattern is obtained by using SAR raw data and transfer function of the system. Two algorithms, namely narrow focusing and wide focusing, are examined for boresight geometry. With the approach used in the study, operation on a certain amount of data set is possible without being have to process the whole data. This is quite advantageous since it provides time efficiency and ability to focus on desired geographical regions. Advantages of this procedure are given and applications to ERS-2 raw data for Istanbul, Turkey are presented.

I. INTRODUCTION

Synthetic aperture radar is a microwave imaging system capable of producing high - resolution images from data collected by a small antenna. The SAR imaging sensor provides information about the surface by measuring and mapping the reflected energy in the microwave region. SAR has unique advantages which make it desirable for monitoring surfaces. It produces high - resolution images independent from sensor altitude. SAR has a day - and – night monitoring capability since it uses active sensors. The active operating mode allows it to be independent from external sources such as sunlight. A cloud – independent nature exists because at microwave frequencies waves can penetrate clouds. Hence, a SAR operating in this frequency range is always able to image the illuminated surface. SAR is mostly used for geological and forest mapping, ocean circulation monitoring, land classification and planet mapping.

In this paper, we present an efficient procedure for processing SAR raw data via two algorithms. We process images to the fullest resolution and we are working on continuous strip – mapping spaceborne SAR. We examine narrow focus and wide focus algorithms to process raw data that is handled and reconstruct images. An important point of view is that we do not have to process all the raw data. With our approach, we are able to process a chosen region in raw data set and operate on that area. It is advantageous since it provides time efficiency and ability to focus on desired geographical regions. Also in narrow focusing case, only a certain part of the image is fully focused. Hence, processing all raw data would not be logical to view only a small well – focused region. Moreover, computer memory problem is generally overcome via working on defined smaller raw data sets.

II. SAR THEORY

The technique of using coherent radar pulses to increase azimuth resolution was invented in 1950s. It was realized that the Doppler frequency shifts of stationary targets with respect to the moving radar sensor could be used to distinguish the different targets that are at the same range distance from the radar.

Consider a radar sensor moving along a straight line as shown in Figure 1. It carries a transmitter that sends out radar waves of wavelength λ, and an antenna that receives the backscattered waves. Suppose it has just transmitted a pulse of radar waves. A target or scatterer that is behind the sensor, for example point C, appears to be moving away from the aircraft. Due to the Doppler effect, it will return a signal that is of lower frequency than the transmitted radar pulse. In contrast, a target that is in front of the sensor, for example point A, will return a signal of higher frequency than that transmitted. Signals from points that are in boresight (i.e. the lines joining these points to the radar are perpendicular to the flight direction), for example point B, will not experience any Doppler shifts.

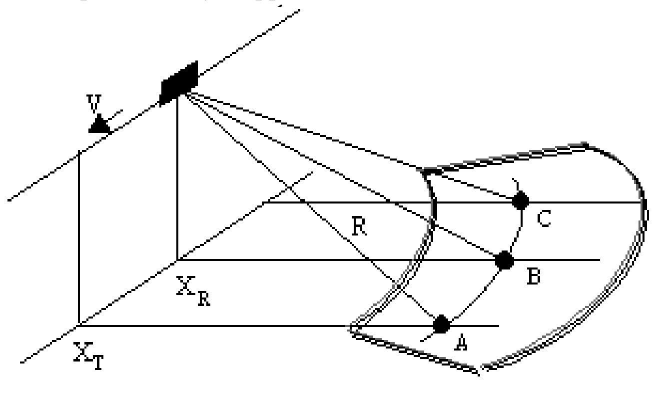

Figure 1. Illustration for Doppler frequency

In the figure, points A, B and C are located at the same range distance R from the radar and so the antenna will simultaneously receive the combined signals of these points (and all other points in the curve). Obviously, it will not be possible to distinguish the points A, B and C from one another, based on only one range measurement. The solution is to combine multiple coherent returns.

Referring to Figure 1, point A is just entering the area illuminated by a radar pulse (illuminated area is shown within the shaded borders). Suppose the speed of the aircraft is V. Then at this instant, the velocity component of this point relative to the aircraft, along the line joining it to the radar antenna is given by;

$$v_r = \frac{V.(x_R - x_T)}{R} \tag{1}$$

x_T and x_R being respectively, the target and radar location along the line of flight ($x_T > x_R$). Due to the Doppler effect, the frequency of the signal from target A differs from that of the transmitted pulse by the following amount:

$$f(x_R) = -\frac{2.v_r}{\lambda} \tag{2}$$

$$f(x_R) = -\frac{2V.(x_R - x_T)}{\lambda.R} \tag{3}$$

This change in radar frequency is called ‘ Doppler frequency ’. It is clear that the Doppler frequency changes with antenna position x_R since x_T is fixed.

In the synthetic aperture technique, the Doppler information of the backscattered wave is used simultanously with the time delay information to generate a high resolution image of the surface being illuminated by the radar. Points equidistant from the radar are located on concentric spheres as given in Figure 2. The backscattered waves from targets along a certain circle will have the same time delay but different Doppler characteristics.

Points distributed on coaxial cones, provide the same Doppler shifts of the backscattered waves but different time delays. Targets on a specific hyperbola, which can be seen in Figure 2, will provide equi- Doppler returns. Thus if the time delay and Doppler information in the backscattered waves are processed simultaneously, the surface can be divided into a coordinate system of concentric circles and coaxial hyperbolas, and each point on the surface can be uniquely identified by a specific time delay and specific Doppler. The resolution capability of the imaging system is thus dependent on the measurement accuracy of the differential time delay and differential Doppler (or phase) between two neighbouring points on the surface.

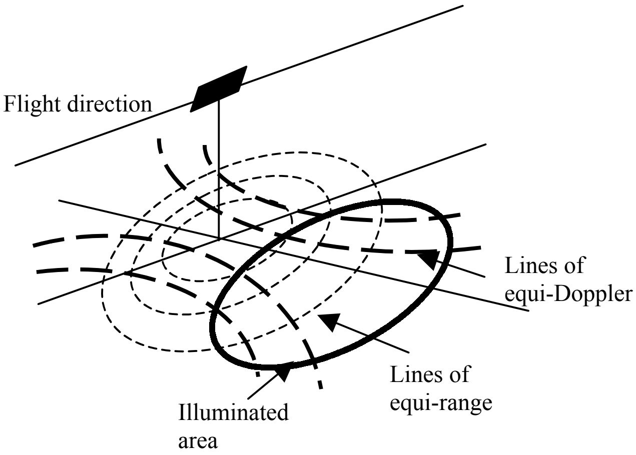

Figure 2. Coordinate system for SAR image formation

The radar sends a pulse to obtain the time delay information. To obtain the Doppler information properly, backscattered waves from many successive pulses are needed with an acceptable pulse repetition frequency (PRF). Hence, as the illuminated areas pass over a certain region, the received signals have a Doppler information and range information for each point on the surface which is illuminated. These information are then processed to identify uniquely each point on the region and generate the image. A large number of operations are needed to generate each pixel in the image.

III. SAR RAW SIGNAL

A. System Characterization

Consider the system geometry given in Figure 3, where the usual cylindrical coordinate system (x, r, θ) is used with its x–axis coincident with the azimuth direction which is assumed to be a straight line. Here, R is the sensor – target distance (range), r is the shortest sensor – target distance and θ is the angle between r and platform trajectory. x_n is the nth position of the real antenna for an 2N+1 equally spaced positions while n = -N,…,N.

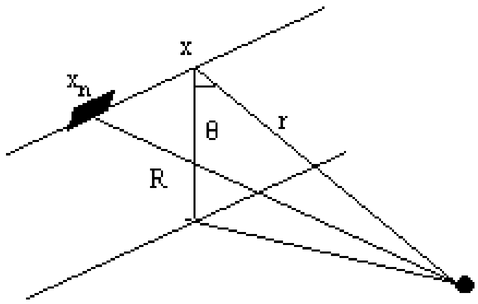

Figure 3. Cylindirical coordinate system geometry

In a SAR system, recorded raw signal *h(.)* can be obtained in terms of impulse response of the system *g(.)*, which is defined as the signal backscattered from a point target, and surface reflectivity pattern γ(.).

$$h(x',r') = \iint \gamma(x,r).g(x'-x,r'-r,r).dx.dr \tag{4}$$

In this proposed system, unprimed coordinates corresponds to ground variables, which are used to locate targets on the ground. Primed variables are called azimuthal variables which are functions of azimuthal time. That is,

$$x' = v.t_n \qquad r' = \frac{c.t'}{2} \tag{5}$$

where

$$t' = t - t_n - 2r/c \tag{6}$$

Equation (4) shows that the SAR imaging problem can be managed by an appropriate filter operation that recovers an estimation of the reflectivity pattern γ(.) starting from the received signal. Thus, we must obtain *g(.)*, to find γ(.), as we already have the raw signal *h(.)* in processing steps. If the dependence of *g(.)*, on r is neglected, (4) can be written as a two – dimensional (2D) convolution:

$$h(x',r') = \iint \gamma(x,r).g(x'-x,r'-r).dx.dr = \gamma(x',r') \otimes g(x',r') \tag{7}$$

In frequency domain;

$$H(\xi,\eta) = \Gamma(\xi,\eta).G(\xi,\eta) \tag{8}$$

where $H(\xi,\eta)$, $\Gamma(\xi,\eta)$ and $G(\xi,\eta)$ are the 2D Fourier transforms (FT) of $h(x',r')$, $\gamma(x',r')$ and $g(x',r')$ respectively. $G(\xi,\eta)$ is called transfer function of the system.

B. ERS-2 Raw Data Set

ERS–2 raw data, which cover a 100 km x 100 km area are processed via different algorithms. Raw data set has 5616x28000 complex samples in range and azimuth directions respectively. In azimuth direction, 28000 pulses are produced to illuminate the region to be imaged. Successive coherent radar returns are received; each backscattered signal is sampled by a suitable sampling frequency and 5616 discrete values are obtained. Obtained data are quantized with 5 bits. Illustration of raw data samples and region of interest is shown in Figure 4 and Figure 5, respectively.

Time difference between any two consecutive azimuth samples is 1/PRF and distance between any two successive azimuth samples is V / PRF. Hence, a uniform sampling is applied in both time and spatial domains for azimuth direction. In range direction, a uniform sampling is performed in time domain while a nonuniform sampling is considered in spatial domain since mapping between time and spatial domains is not linear. For example, ground distance between two successive spatial samples nearest to the sensor for a particular beam is 17 m while the last two samples are separated with 23 m.

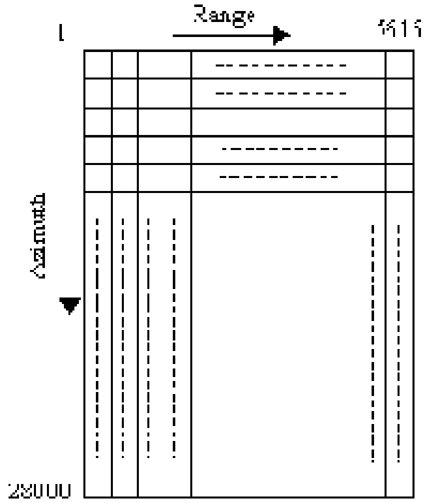

Figure 4.Schematic diagram of raw data array

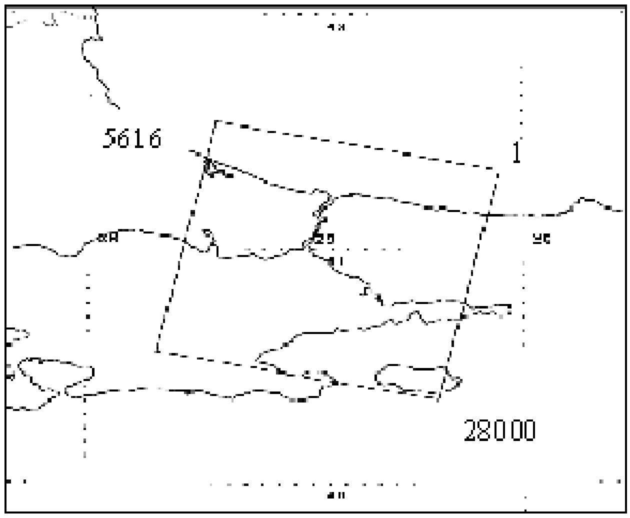

Figure 5. Geographical region of interest

IV. PROCESSING PROCEDURE

A. Narrow Focusing

In narrow focus processing scheme, range dependence of the transfer function is neglected. Let us have $r=r_0$ in (4), where r_0 is the range distance to the center of the chosen area to be imaged. In this case Eq. 4 becomes;

$$h(x',r') = \iint \gamma(x,r).g(x'-x,r'-r,r_0).dx.dr \tag{9}$$

This expression corresponds to a 2D convolution and SAR data processing a 2D deconvolution. It is convenient to carry out the deconvolution operation in the Fourier domain since it provides computational efficiency. We recast (9) according to (4) such that;

$$H(\xi,\eta)=\Gamma(\xi,\eta).G_0(\xi,\eta) \tag{10}$$

$G_0(\xi,\eta)$ is the 2D Fast Fourier Transform (FFT) of $g(x',r',r_0)$. We can write $\Gamma(\xi,\eta)$ approximately as

$$\Gamma(\xi,\eta)= H(\xi,\eta).G_0^*(\xi,\eta) \tag{11}$$

The block diagram of the 2D processing algorithm based on (11) is given in Figure 6 and narrow focus result for the Bosphorus, Istanbul is shown in Figure 7. The key point of the procedure is represented by knowledge of the transfer function by assuming $r = r_0$. For this reason this procedure is referred as the narrow focusing since only the central part of the scene $r = r_0$ is perfectly focused. Before taking 2D FFT^{-1}, Hamming window is applied to data to have a better performance on the reconstructed image.

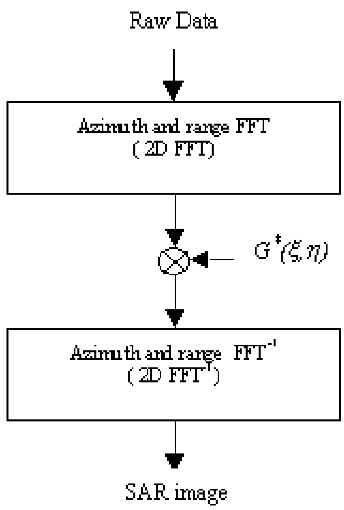

Figure 6. Narrow focus processing steps

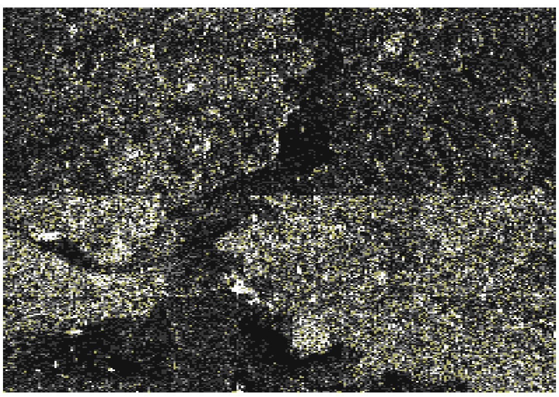

Figure 7. Narrow focus result for the Bosphorus, Istanbul (4x1024x1024 samples)

B. Wide Focusing

Narrow focus processing procedure does not account for range dependence of the transfer function; this is not acceptable in many cases and ways to obtain fully focused image are desirable. This implies moving from a narrow focus to a wide focus processor. In order to compansate imperfections caused by phase variations with changing range, a ξ - dependent μ term is introduced:

$$\mu(\xi)= -\frac{2.a}{r_0}.\left(\frac{L}{\lambda}\right)^2 + \frac{L}{\lambda.r_0}.\sqrt{\left(2.a.\frac{L}{\lambda}\right)^2 - \xi^2} \tag{12}$$

where L is the real aperture length and a is defined such that;

$$a = \frac{2.\pi.\lambda.r_0}{L^2} \tag{13}$$

It can be seen that varies symmetrically; it means a symmetrical phase correction, which is minimum at the image center and increasing towards edges in azimuth direction, is applied on the image. Variation of μ as a function of number of samples in azimuth direction (n) for r_0 = 846417 m, a = 3010, L = 10 m and λ = 0.0566 m for a 1024x1024 data region is given in Figure.8.

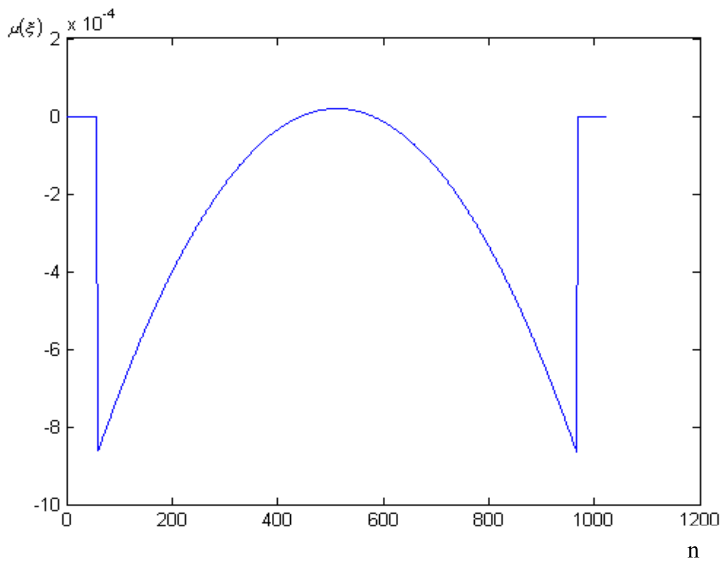

Figure 8. μ as a function of n

Wide focus processing steps are shown in Figure 9 and result for the Bosphorus, Istanbul is obtained as seen in Figure 10. A focus which spreads over the whole image and differs from narrow focusing is recognized. Note that Hamming window is used in ξ domain before ξ - FFT $^{-1}$.

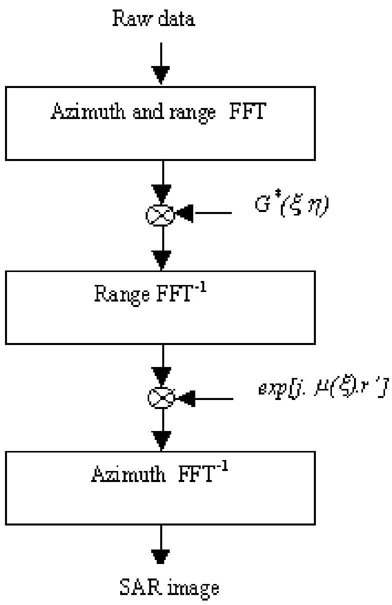

Figure 9. Wide focus processing steps

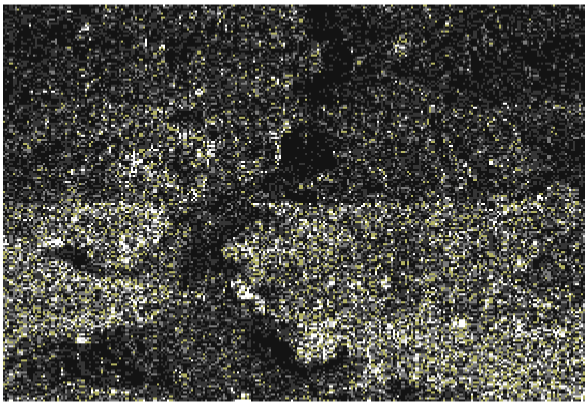

Figure 10. Wide focus result for the Bosphorus, Istanbul (4x1024x1024 samples)

V. CONCLUSION

In this study, an investigation is carried out on SAR raw data processing. Facilities of narrow focus and wide focus algorithms are examined. These algorithms provide efficent results although some aberrations exist in the nature of the processing schemes. Transfer function of the system, which is quite important during process, is obtained. Operations applied are not for perfect geometries since some approximations are considered. ERS-2 raw data for Istanbul, Turkey are used to compare performances of the algorithms. Images of certain chosen parts of raw data are obtained as the chance to process all the raw data is possible as well.

REFERENCES

1. Franceschetti, G. and Lanari R., Synthetic Aperture Radar Processing, CRC Press, 1999..
2. Curlander, J.C. and McDonough, R.N., Synthetic Aperture Radar: Systems and Signal Processing,Wiley&Sons, 1991.
3. Wehner, D.R., High Resolution Radar, Artech House, 1995.
4. Goj, W.W., Synthetic Aperture Radar and Electronic Warfare, Artech House, 1993..
5. Morchin W., Radar Engineer' s Sourcebook, Artech House, 1993.
6. Mensa,.High Resolution Radar Imaging, Artech House, 1981.
7. Elachi C., Bicknell T., Jordan R.L. and Wu C., Spaceborne Synthetic– Aperture Imaging Radars: Applications, Techniques and Technology, Proceedings of the IEEE, Vol.70, pp.1174 – 1209, 1982..
8. Tomiyasu K., Tutorial Review of Synthetic Aperture Radar with Applications to Imaging of the Ocean Surface, Proceedings of the IEEE, Vol.66, pp.563 – 572, 1978..
9. Munson D.C. and Visentin R.L., A Signal Processing View of Strip–Mapping Synthetic Aperture Radar, IEEE Transactions on Acoustics, Speech and Signal Processing, Vol.37, pp.2131 – 2147, 1989.
10. Franceschetti G., Migliaccio M., Riccio D.. Schirinzi G., SARAS: A Synthetic Aperture Radar (SAR) Raw Signal Simulator, IEEE Transactions on Geoscience and Remote Sensing, Vol.30, pp.110- 113, 1992.
11. Francheschetti G., Lanari R. and Marzouk E.S., Aberration free SAR Raw Data Processing via Transformed Grid Predeformation, IGARSS' 93, Vol.4, pp.1593 – 1595, 1993.
12. Berardino P., Marrazzo M., Migliaccio M., Lanari R., ERS-1 / 2 and IFSAR for Antarctica, IGARSS'01, Vol.6, pp. 2554 – 2556, 2001.
13. Curlander J.C., Utilization of Spaceborne SAR Data for Mapping, IEEE Transactions on Geoscience and Remote Sensing, Vol.22, pp.106 – 112, 1984..
14. Freeman A., Johnson W.T.K., Huneycutt B., Jordan R., Hensley S., Siouera P., Curlander J.C., The ' Myth ' of the Minimum SAR Antenna Area Constraint, IEEE Transactions on Geoscience and Remote Sensing, Vol.38, pp.320 – 324.
15. Bamler R., A Comparison of Range – Doppler and Wavenumber Domain SAR Focusing Algorithms, IEEE Transactions on Geoscience and Remote Sensing, Vol.30, pp.706 – 713, 1992.
16. Bamler R. and Runge H., PRF – Ambiguity Resolving by Wavelength Diversity, IEEE Transactions on Geoscience and Remote Sensing, 1991. Vol.29, pp.997 – 1001, 1991.
17. Li F.K. and Johnson W.T.K., Ambiguities in Spaceborne Synthetic Aperture Radar Data, IEEE Transactions on Aerospace and Electronic Systems, Vol.19, pp.389–395, 1983..
18. Madsen S.N., Estimating the Doppler Centroid of SAR Data, IEEE Transactions on Aerospace and Electronic Systems, Vol.25, pp.134 – 139, 1989.
19. Moreira A., Suppressing the Azimuth Ambiguities in Synthetic Aperture Radar Images, IEEE Transactions on Geoscience and Remote Sensing, Vol.31,pp. 885 – 888, 1993.